Three-Dimensional Structure of Ribonuclease T_1 Complexed with an Isosteric Phosphonate Substrate Analogue of GpU: Alternate Substrate Binding Modes and Catalysis[†,‡]

Raghuvir K. Arni,*[,§] Leandra Watanabe,[§] Richard J. Ward,[||] Robert J. Kreitman,[⊥] Kapil Kumar,[▽] and Frederick G. Walz, Jr.*[,▽]

Department of Physics, UNESP/IBILCE, S. J. do Rio Preto-SP, CEP 15054−000, CP 136, Brazil, Department of Biochemistry, USP/FMRP, Avenida Bandeirantes 3900, BR-14049900 Ribeirao Preto, SP, Brazil, Laboratory of Molecular Biology, Division of Basic Sciences, National Cancer Institute, National Institutes of Health, 3714E16, 37 Convent Drive, MSC 4255, Bethesda, Maryland 20892, and Department of Chemistry, Kent State University, Kent, Ohio 44242

Received November 3, 1998; Revised Manuscript Received December 29, 1998

ABSTRACT: The X-ray crystal structure of a complex between ribonuclease T_1 and guanylyl(3′-6′)-6′-deoxyhomouridine (GpcU) has been determined at 2.0 Å resolution. This ligand is an isosteric analogue of the minimal RNA substrate, guanylyl(3′−5′)uridine (GpU), where a methylene is substituted for the uridine 5′-oxygen atom. Two protein molecules are part of the asymmetric unit and both have a GpcU bound at the active site in the same manner. The protein−protein interface reveals an extended aromatic stack involving both guanines and three enzyme phenolic groups. A third GpcU has its guanine moiety stacked on His92 at the active site on enzyme molecule A and interacts with GpcU on molecule B in a neighboring unit via hydrogen bonding between uridine ribose 2′- and 3′-OH groups. None of the uridine moieties of the three GpcU molecules in the asymmetric unit interacts directly with the protein. GpcU−active-site interactions involve extensive hydrogen bonding of the guanine moiety at the primary recognition site and of the guanosine 2′-hydroxyl group with His40 and Glu58. On the other hand, the phosphonate group is weakly bound only by a single hydrogen bond with Tyr38, unlike ligand phosphate groups of other substrate analogues and 3′-GMP, which hydrogen-bonded with three additional active-site residues. Hydrogen bonding of the guanylyl 2′-OH group and the phosphonate moiety is essentially the same as that recently observed for a novel structure of a RNase T_1−3′-GMP complex obtained immediately after in situ hydrolysis of *exo*-(S_p)-guanosine 2′,3′-cyclophosphorothioate [Zegers et al. (1998) *Nature Struct. Biol. 5*, 280−283]. It is likely that GpcU at the active site represents a nonproductive binding mode for GpU [Steyaert, J., and Engleborghs (1995) *Eur. J. Biochem. 233*, 140−144]. The results suggest that the active site of ribonuclease T_1 is adapted for optimal tight binding of both the guanylyl 2′-OH and phosphate groups (of GpU) only in the transition state for catalytic transesterification, which is stabilized by adjacent binding of the leaving nucleoside (U) group.

Ribonuclease T_1 (RNase T_1)[1] is an extracellular enzyme from *Aspergillus oryzae* that catalyzes the hydrolysis of RNA at guanylyl residues yielding new guanosine 3′-phosphate and 5′-OH ends. This occurs in a two-step process with cleavage of the RNA chain by transesterification of a 5′-phosphoester bond to form a guanosine 2′,3′-cyclic phosphate terminus in the first step followed by hydrolysis of the cyclic phosphate to form a guanosine 3′-phosphate in a second, independent step. This stable, low molecular weight, monomeric endonuclease is the leading representative of a family of related fungal/bacterial proteins that share sequence and three-dimensional structural similarities (*1*−*3*). Even though RNase T_1 has been extremely well characterized, the determination of a definitive catalytic mechanism has been elusive. Nevertheless, it is known that contributing residues at its catalytic site include Tyr38, His40, Glu58, Arg77, His92, and Phe100 and, with the exception of Arg77, the importance of these residues in catalysis was verified by site-directed mutagenesis (*3*). It is generally agreed that the α-carboxylate group of Glu58 acts as a general base and

[†] This work was supported in part by FAPESP and CNPq (Brazil).

[‡] Refined coordinates and structure factors have been deposited in the Brookhaven Protein Data Bank: PDB ID code 1B2M.

* Corresponding author: Tel (330) 672-2493; FAX (330) 672-3816; Email FWALZ@KENT.EDU.

[§] Department of Physics, UNESP/IBILCE.

[||] Department of Biochemistry, USP/FMRP.

[⊥] National Cancer Institute, NIH.

[▽] Kent State University.

[1] Abbreviations: 3′-CMP, cytidine 3′-phosphate; GfpC, 2′-deoxy-2′-fluoroguanylyl(3′−5′)cytidine; 3′-dGMP, 2′-deoxyguanosine 3′-phosphate; 3′-dUMP, 2′-deoxyuridine 3′-phosphate; 3′-GMP, guanosine 3′-phosphate; GpcC, guanylyl(3′−6′)-6′-deoxyhomocytidine; GpcU, guanylyl(3′−6′)-6′-deoxyhomouridine; GpG, guanylyl(3′−5′)guanosine; GpU, guanylyl(3′−5′)uridine; G2′p5′G, guanylyl(2′−5′)guanosine; dCpdA, deoxycytidylyl(3′−5′)deoxyadenosine; dGpdC, deoxyguanylyl-(3′−5′)deoxyctidine; NMR, nuclear magnetic resonance; 2′-OH, 2′-hydroxyl; RNase, ribonuclease; rms, root-mean-square; RNase S, a fully active cleavage product of RNase A where the peptide bond between residues 20 and 21 was hydrolyzed by mild digestion with subtilisin; SD, standard deviation; TBP, trigonal bipyramidal phosphorane; 3′-UMP, uridine 3′-phosphate; UpcA, uridylyl(3′-6′)-6′-deoxyhomoadenosine.

10.1021/bi982612q CCC: $18.00
Published on Web 02/04/1999

the β-imidazolium group of His92 acts as a general acid in a concerted action for enzyme-catalyzed transesterification (*3*−*5*). It is also likely that the side chains of Tyr38, Arg77, and Phe100 are mainly involved in the electrostatic stabilization of a trigonal bipyramidal phosphorane (TBP) transition state, whereas the role of His40 in catalysis is less clear (*3*). The results of four independent reports on crystal structures of RNase T_1 complexed with 3′-GMP showed that His40 formed a strong hydrogen bond with the ribose 2′-OH group, which was also hydrogen-bonded with Glu58 (*6*−*9*). On the basis of these observations, it was proposed that the imidazolium group of His40 either electrostatically stabilizes the negative charge on the 2′-oxygen that develops with proton transfer to the carboxylate of Glu58 (*6*) or polarizes the 2′-OH group to facilitate this proton transfer in the first step of the reaction with RNA (*7*). However, evidence for a hydrogen bond between His40 and the 2′-OH group in RNase T_1 complexes with GpN (N = A, C, G, or U) phosphodiester substrates or substrate analogues has not been reported.

A kinetic model to explain the dramatic effect of the leaving nucleoside group (i.e., N in GpN substrates) on k_{cat} proposed tight enzyme binding with the guanosine moiety such that an initial, catalytically incompetent enzyme−substrate complex only involves interactions with this portion of the substrate (*3*). This initial complex then isomerizes to a catalytically productive mode where both nucleoside moieties specifically interact with the enzyme. This elegant model fits all the data but the discrete nature of the two binding modes is unknown. Therefore, it would be useful to study structures of enzyme complexes with nonreactive analogues of GpN substrates to elucidate different binding modes regarding the occupancy of previously defined subsites.[2]

The crystal structure of RNase T_1 complexed with G2′p5′G had the 5′-end guanine at the primary recognition (guanine) site and the 3′-end guanine at the N1 subsite where it was stacked on the imidazolium ring of His92 (*12*). RNase Ms is an excellent structural model for RNase T_1 and the structure of this orthologous enzyme complexed with GfpC (a nonreactive substrate analogue of GpC having a fluorine substituting for the guanosine 2′-OH group) revealed a similar binding at the G (guanine), p1, and N1 subsites (*13*). NMR studies on the binding of GfpU with RNase T_1 indicated that the guanosine and uridine moieties interacted with the enzyme (*14*). On the other hand, the crystal structure of orthologous barnase complexed with dGpdC indicated that this substrate analogue was not optimally bound at the active site and made contacts with neighboring molecules (*15*). In all of these cases, the bound substrate analogues did not contain a 2′-OH group, which precluded information regarding its interactions with the enzyme. A complementary approach to these studies employed an isosteric phosphonate analogue of GpU having a methylene substitution for the 5′-phosphoryl oxygen (designated GpcU), which has a guanosine 2′-OH group. NMR studies on the binding of GpcU with RNase Pb_1 (another RNase T_1 orthologue) were reported; however, unlike the case for GfpU with RNase T_1 (*14*), the uridine moiety was not bound to the enzyme (*16*).

We also prepared GpcU and determined that $\Delta G°$ for its binding with RNase T_1 was less negative than that for GpU by only 0.4 kcal/mol, which suggested that its interactions with the enzyme closely approximate those for a minimal RNA substrate (*17*). We now report the X-ray crystal structure of a RNase T_1−GpcU complex. Two protein molecules are part of the asymmetric unit and both have GpcU bound essentially in the same manner at the active site. A third GpcU has its guanine moiety at the N1 subsite on one enzyme molecule and interacts with another GpcU on a symmetry-related molecule via hydrogen bonding between uridine ribose moieties. Some key findings regarding interactions at the active site are that the guanosine 2′-OH group is tightly bound to His40 and Glu58, that the phosphonate group is only bound with Tyr38, and that the uridine moiety does not contact the enzyme.

MATERIALS AND METHODS

Preparation of GpcU. GpcU was prepared by condensing N^2-benzoyl-5′-*O*-(dimethoxytrityl)guanosine (1.5 mmol) with pyridinium-2′,3′-*O*-isopropylidene-6′-deoxyhomouridine 6′-phosphonate (1.2 mmol) using dicyclohexylcarbodiimide according to the method of Jones et al. (*18*). The reported synthesis of 2′,3′-*O*-isopropylidene-6′-deoxyhomouridine 6′-phosphonate (*19*) was followed with modifications used in the synthesis of the 6′-phosphonate analogue of 5-fluorodeoxyuridylate (*20*). The protected guanosine was produced by synthesizing N^2,2′,3′,5′-tetrabenzoylguanosine (*21*) followed by partial deblocking to N^2-benzoylguanosine (*22*). N^2-Benzoyl-5′-*O*-(di-*p*-methoxytrityl)guanosine was then prepared according to the synthesis of 5′-*O*-(di-*p*-methoxytrityl)-N^4-benzoylcytidine (*23*). After condensation, the deprotected products [guanylyl(3′−6′)-6′-deoxyhomouridine and guanylyl(2′−6′)-6′-deoxyhomouridine; 80% yield] were separated on a DEAE Sephadex A-25 column (2.6 × 60 cm) by using an 8 L linear gradient of ammonium bicarbonate (pH 8.5) from 0.02 to 0.16 M at a flow rate of 1.3 mL/min at room temperature. Treatment of the 2′-isomer with 20% acetic acid at 100 °C for 15 min resulted in its equilibration with the 3′-isomer (slightly favored), which was chromatographically purified to increase the yield of the desired product.

GpcU binding with RNase T_1. Ribonuclease T_1 (Gln25 allozyme) was purified as previously described and its concentration was determined with a molar absorptivity at 278 nm ($\epsilon_{278\ nm}$) of 2.1×10^4 M^{-1} cm^{-1} (*24*). The concentration of GpcU was determined with the molar absorptivity for GpU [$\epsilon_{280\ nm} = 1.06 \times 10^4$ M^{-1} cm^{-1} (*25*)]. Binding was studied at pH 5.5 using ultraviolet difference spectroscopy (*24*). The maximum difference absorbance occurred at 291 nm and values of the difference absorbance, ΔA, at this wavelength were determined for a fixed total concentration of the enzyme ($[E]_0 = 3.43 \times 10^{-3}$ M) in the presence of variable total concentrations of GpcU ($[L]_0$; (0.479−2.21) $\times 10^{-4}$ M). The equilibrium is characterized by $K_d = \{([E]_0 - \Delta A/\Delta\epsilon)([L]_0, - \Delta A/\Delta\epsilon)\}/(\Delta A/\Delta\epsilon)$ where K_d is the dissociation constant, $\Delta\epsilon$ is the difference molar absorptivity at 291 nm and $\Delta A/\Delta\epsilon$ = [EL] (the concentration of the enzyme−ligand complex). Data were fit to the quadratic

[2] Nomenclature for subsites on RNase T_1 can be summarized in terms of the generalized RNA sequence 5′-2p·1N·1p·G·p1·N1·p2-3′, where G represents the primary recognition site for guanosine, p1 is the binding/catalytic site engaging the guanosine 3′-phosphodiester group, N1 is the site occupied by the leaving nucleoside group, etc. (*10*, *11*).

solution, $\Delta A = \Delta\epsilon\{([L]_0 + [E]_0 + K_d - (([L]_0 + [E]_0 + K_d)^2 - 4[L]_0[E]_0)^{1/2})/2\}$ using NFIT as previously described (*26*).

Crystallization. The protein was dissolved in 10 mM sodium acetate, pH 4.1, at a concentration of 10 mg/mL. GpcU was added at a molar excess of 1.2:1 and incubated at 4 °C for 24 h. Crystallization trials used the hanging-drop vapor-diffusion technique (*27*) with 24-well tissue culture plates. A 2 μL droplet of the protein−ligand solution was mixed with an equal volume of reservoir solution [0.1 M Tris-HCl, 0.2 M magnesium chloride, and 30% poly(ethylene glycol) 4000 at pH 8.75]. Initial crystallization trials used screening conditions (*28*) at room temperature. A single crystal with dimensions of 0.2 × 0.2 × 0.15 mm was obtained after 6 weeks of incubation in the presence of the reservoir solution.

Data Collection. Cu Kα radiation was produced by a Rigaku RU200 rotating anode generator operating at 50 kV and 100 mA using a fine focus filament (0.3 mm) and a crystal monochromator. Diffraction intensities were measured with a Rigaku R-Axis IIC imaging plate detector. The crystals belong to space group $P2_12_12_1$ with cell constants $a = 69.91$ Å, $b = 90.29$ Å, and $c = 33.98$ Å; a complete data set was collected to 2.0 Å at 22 EC. The data were processed using the Rigaku Data Processing Package, PROCESS (*29*), to provide an R_{sym} of 6.4%.

Structure Determination and Refinement. The atomic coordinates of RNase T_1 in an enzyme−2′-GMP complex [PDB code 1rnt (*30*)] stripped of solvent and with an overall temperature factor of 20 Å^2 were used as the search model for molecular replacement using AMORE (*31*). The self-rotation function indicated the presence of two protein molecules in the asymmetric unit. The cross-rotation function using data in the resolution range 20.0−3.5 Å (correlation coefficient = 19.6/16.1) and translation function (resolution range 8.0−3.5 Å) determined the positions for the two molecules in the asymmetric unit (correlation coefficient = 59.1; *R*-factor = 38.6%). The rigid body refinement using data between 8.0 and 3.5 Å led to a correlation coefficient of 69.0 and an *R*-factor of 32.9%. Simulated annealing, positional, overall anisotropic *B*-factor, and individual restrained *B*-factor refinements were performed with X-PLOR version 3.1 (*32*). For model building, the program O (*33*) was used on a Silicon Graphics Extreme workstation. A number of omit maps were calculated and clear electron density was observed for the three GpcU molecules at all stages of the refinement. The refinement converged to a crystallographic residual of 18.7% (R_{free} = 25.4%) for data between 8.0 and 2.0 Å. An analysis of the Ramachandran plot by PROCHECK (*34*) indicated that 90.7% of the residues lie in the most favored regions and 9.3% of the residues lie in additionally allowed regions. The rms deviations from ideal values for the final model indicates good stereochemistry. The final model consists of 1556 protein atoms, 120 ligand atoms, and 92 solvent molecules. Data collection, molecular replacement, and refinement statistics are summarized in Table 1.

Table 1: Data Collection, Molecular Replacement, and Refinement Statistics

Data Collection	
max. resolution (Å)	2.0
R_{sym} (%)	6.4
space group	$P2_12_12_1$
cell constants (Å)	$a = 69.91$, $b = 90.29$, $c = 33.98$
Molecular Replacement	
rotation	
resolution range (Å)	20.0−3.5
correlation coefficient	19.6/16.1
translation	
resolution range (Å)	8.0−3.5
correlation coefficient	59.1
R-factor (%)	38.6
rigid-body refinement	
resolution range (Å)	8.0−3.5
correlation coefficient	69.0
R-factor (%)	32.9
Refinement Statistics	
total reflections accepted	26 734
resolution range (Å)	8.0−2.0
σ cutoff	2.0
F^2/σ (overall)	7.4
F^2/σ (last shell 2.0−2.2 Å)	3.6
completeness in last shell (%)	69.5
R (%)	18.7
R_{free} (%)	25.4
rms deviation bonds (Å)	0.011
rms deviation angles (deg)	1.742
rms deviation impropers (deg)	1.420

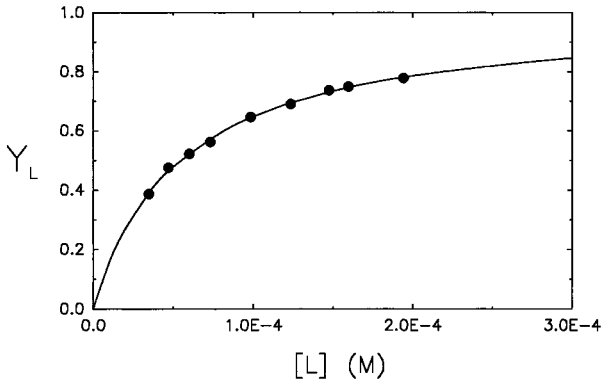

FIGURE 1: Plot of the fractional saturation, Y_L, for GpcU binding with RNase T_1 vs free ligand concentration at 25 °C and pH 5.5. Experimental values of Y_L were calculated as $(\Delta A/\Delta\epsilon)/[E]_0$ and corresponding values of [L] as $[L]_0 - [EL]$, where $[EL] = \Delta A/\Delta\epsilon$. The theoretical curve was calculated from $Y_L = [L]/([K_d + [L])$.

RESULTS

GpcU Binding with RNase T_1. Excellent agreement was found between the binding data and the model quadratic equation (see under Materials and Methods) where $r^2 = 0.9999$ and the best-fit values for K_d and $\Delta\epsilon$ were $(1.85 \pm 0.07) \times 10^{-4}$ M and 3633 ± 47 M^{-1} cm^{-1}, respectively. A plot of the fractional saturation as a function of the free GpcU concentration is shown in Figure 1. The free energy change for binding was −5.8 kcal/mol [$\Delta G^\circ = -RT \ln (1/K_d)$], which was 0.4 kcal/mol less negative than that calculated for GpU [$\Delta G^\circ = -RT \ln (1/K_M)$] using the Michaelis constant, K_M, which was determined under essentially the same conditions (*35*).

Structural Overview. The asymmetric unit of the crystal consists of two RNase T_1 and three GpcU molecules, which are arranged as shown in Figure 2. Protein molecule A has one ligand with its guanine bound at the primary recognition site (GpcU1) and another ligand with its guanine at the N1 subsite (GpcU3). Protein molecule B has only one bound

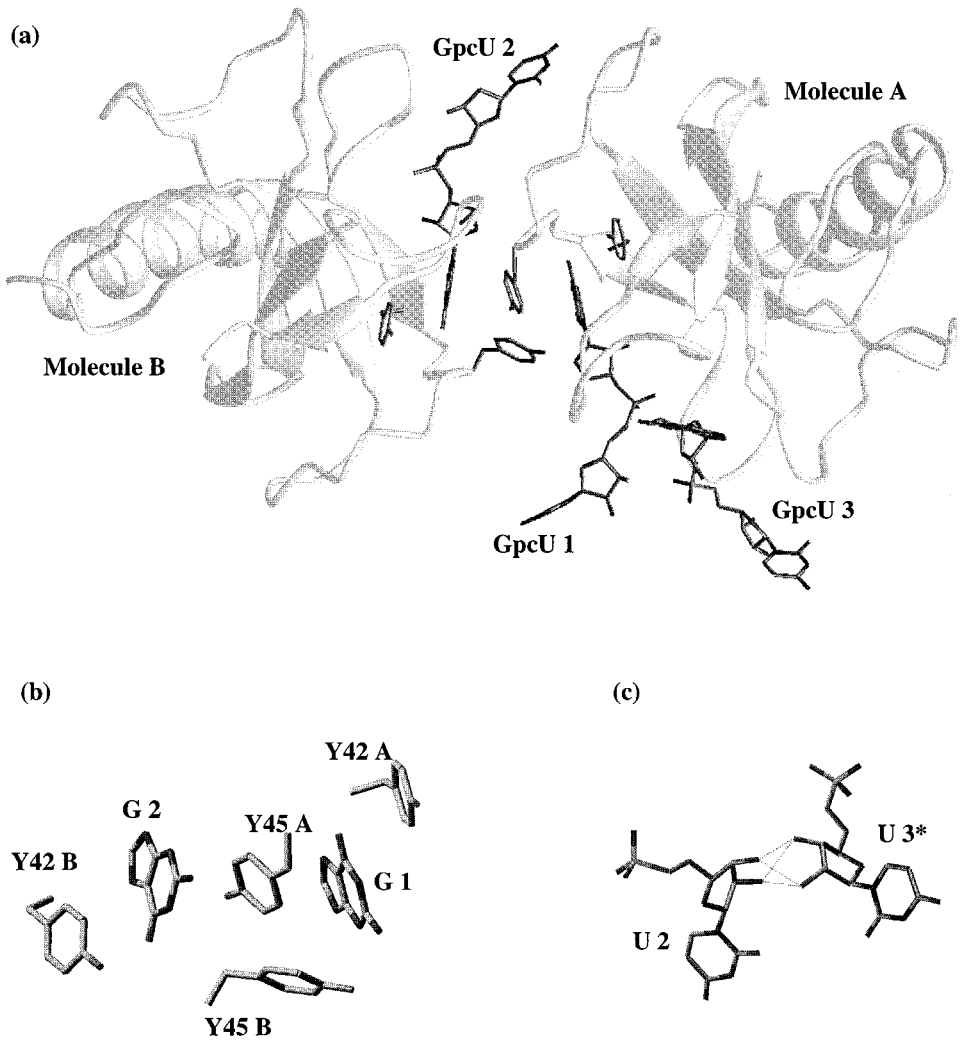

FIGURE 2: View of the two RNase T_1 molecules and three GpcU molecules in the asymmetric unit. (a) View of RNase T_1 molecule A complexed with GpcU1 and GpcU3 with RNase T_1 molecule B complexed with GpcU2. (b) Detail of the extended aromatic stack at the dimeric interface where G1 and G2 are the guanine moieties of GpcU1 and GpcU2, respectively; and Y42A, Y45A, Y42B, and Y45B are phenolic groups of tyrosine 42 and 45 on molecules A and B, respectively. (c) Hydrogen bonds between the ribose 2′-OH and 3′-OH groups of uridine residues for GpcU2 (U2) of one asymmetric unit with UpcU3 ($U3^*$) of an adjacent symmetry-related unit; dotted lines represent hydrogen bonds.

ligand (GpcU2) with its guanine at the primary recognition site. None of the uridine moieties interacts with either protein molecule, but the uridine 2′- and 3′-hydroxyls of GpcU3 hydrogen-bond with the same groups on GpcU2 from a symmetry-equivalent unit in the crystal with four donor−acceptor oxygen distances ranging from 2.55 to 2.77 Å as shown in Figure 2C. Also, the uridine 3′-OH of GpcU1 forms a hydrogen bond with O1P (the *pro-S* phosphinic oxygen) of GpcU3 (2.93 Å). In addition, a water molecule forms a strong hydrogen bond with O1P of GpcU1 (2.66 Å) but a comparable, fixed water was not associated with GpcU2 at the active site of protein molecule B. This water molecule is also within hydrogen-bonding distance with the side chains of Glu58 (3.08 Å), Arg77 (3.57 Å) and His92 (3.55 Å).

The dimer interface, which involves essentially homologous protein surfaces including the primary recognition site, is different from those for other dimeric forms of crystalline RNase T_1, which exhibit heterologous interactions. It includes an extended stack of five aromatic groups which proceeds as Y42(molecule A)−Gua(GpcU1)−Y45(molecule A)−Gua-(GpcU2)−Y42(molecule B) as illustrated in Figure 2B. This array is accommodated by movement of Tyr45 in molecule B. Superpositioning of α-carbons for the two protein molecules yielded an rms deviation of 0.4 Å. Figure 3 illustrates the superpositioning of the active-site−ligand regions.

Comparisons with 3′-GMP−RNase T_1 Complexes. Protein interactions with the guanosine moiety of GpcU at the active site are similar to those observed in RNase T_1−3′-GMP complexes (*6*−*9*). Hydrogen bonds with guanine at the primary recognition site involving Asn43, Asn44, Tyr45, Glu46, and Asn98 were essentially identical for both ligands (data not shown). Also, all GpcU and 3′-GMP complexes had similar hydrogen bonds for His40 and Glu58 with the guanosine 2′-OH group; Tyr38 with a nonbridging phosphinic oxygen; and main-chain (O) to side-chain (N−H) hydrogen bonds that conformationally stabilize His40, Arg77, and His92 (see Table 2). On the other hand, side-chain to side-chain hydrogen bonds between Tyr38 and Asn36 were only observed in the GpcU1 and GpcU2 complexes. In most 3′-GMP−RNase T_1 complexes the phosphomonoester group completely occupies the p1 subsite, where it closely interacts with Tyr38, Arg77, His92, and Phe100; but this is not case for GpcU1 and GpcU2 as well as one 3′-GMP complex (*9*),

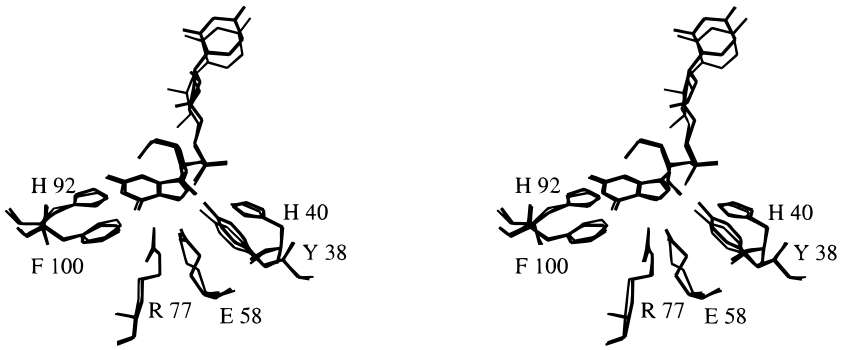

FIGURE 3: Superpositioning of GpcU1 and GpcU2 with active-site residues (Tyr38, His40, Glu58, Arg77, His92, and Phe100) on RNase T_1 molecules A and B.

Table 2: Selected Hydrogen-Bond Distances (≤3.5 Å) for Active-Site Groups in Complexes of RNase T_1 with GpcU and 3′-GMP

donor		acceptor[a]		distance (Å)				
residue	atom	residue	atom	GpcU1	GpcU2	3′-GMP[b] (site A)	3′-GMP[c] (site A)	3′-GMP[d] (site B)
Asn36	ND2	Tyr38	OH	3.13	3.20			
Tyr38	OH	Gp	(P)O	2.43	2.71	2.53 ± 0.04	2.30	2.80
His40	ND1	Asn36	O	3.09	2.92	2.84 ± 0.04	2.98	2.96
His40	ND1	Ser37	O	2.67	2.79	2.94 ± 0.11	2.84	2.84
His40	NE2	Gp	2′O	2.56	2.54	2.64 ± 0.06	2.48	2.56
Gp	2′O	Glu58	OE1	2.52	2.60	2.62 ± 0.08	2.95	2.66
Arg77	NE	Glu58	OE1	3.29	2.81	3.11 ± 0.19	3.20	3.11
Arg77	NH2(1)	Gp	(P)O			3.00 ± 0.21	3.43	
Arg77	NH1(2)	Gly74	O	2.66	3.09	2.99 ± 0.10	2.16	2.97
Arg77	NH1(1)	Asp76	O	3.01	2.84	2.97 ± 0.05	2.86	2.99
His92	ND1	Asn99	O	2.81	2.86	2.74 ± 0.02	2.85	2.86
His92	NE2	Gp	(P)O			2.75 ± 0.27	2.60	

[a] (P)O is a nonbridging oxygen bound to phosphorus. [b] Average ± SD for conformations of 3′-GMP with the phosphate group at site A (*9*); PDB codes 1rga (*6*), 1rgc (*7*), and 1rls (*8*). [c] Conformation of 3′-GMP with the phosphate group at site A; PDB code 6gsp (*9*). [d] Conformation of 3′-GMP with the phosphate group at site B; PDB code 4gsp (*9*).

where the phosph(on)ate groups partially occupy this subsite having a single hydrogen bond with Tyr38. The different interaction loci for the phosphomonoester group in these alternate positions were referred to as site A (complete occupation of the p1 subsite) and site B (partial occupation of the p1 subsite) (*9*).[3]

The guanosine glycosidic torsion angle (χ) narrowly ranged from 44° to 63° for all 3′-GMP and GpcU complexes at the active site of RNase T_1. Similar ribose conformations with pseudorotational angles (*P*) ranging from 51° to 96° ($C_{4'}$-*exo* to $O_{4'}$-*endo*) were observed for 3′-GMP complexes, which have their phosphate groups at site A (*6*−*9*). On the other hand, *P* closely ranged from 161° to 180° (∼$C_{2'}$-*endo*) for GpcU1/GpcU2 and 3′-GMP, where the phosph(on)ate groups occupy site B (*9*). Superpositioning of either GpcU1 or GpcU2 with 3′-GMP occupying phosphate site B, showed near congruence for their guanylyl moieties and placed their phosphorus atoms less than 0.9 Å apart (data not shown).

[3] Crystal structures were determined for *exo*-(S_p)-guanosine 2′,3′-cyclophosphorothioate complexed with RNase T_1 and during the course of its slow hydrolysis to guanosine 3′-thiophosphate, which is rapidly desulfurized to 3′-GMP (*9*). The conformation of the initial 3′-GMP product had its phosphate group positioned for hydrogen bonding only with Tyr38 (site B). Subsequently, the conformation of nucleotide changes so that the phosphate group also interacts with Arg77, His92, and Phe100 in addition to Tyr38 (site A). [This latter structure was previously found for directly prepared crystals of the 3′-GMP−RNase T_1 complex (*6*−*8*).] Specific hydrogen bonds with the guanine and guanosine 2′-OH moieties were maintained in the initial and final binding modes of 3′-GMP. It was also noted that the residues involved in phosphate group binding occupied fixed positions regardless of covalent and conformational changes in the bound nucleotide (*9*).

Comparisons with Dinucleoside Monophosphate−*RNase T_1 Complexes.* G2′p5′G and GfpC, which lack a ribose 2′-OH on the 5′-end guanine nucleoside, adopt glycosidic and backbone conformations that permit their phosphodiester groups to completely interact at the p1 subsite (site A) with Tyr38, Glu58, Arg77, His92, and Phe100 (*12*, *13*) like the phosphomonoester groups of 3′-GMP in most complexes (see above). Superpositioning of active-site residues for RNase T_1−GpcU (molecule A with GpcU1 and GpcU3), RNase T_1−G2′p5′G, and RNase Ms−GfpC complexes gave the results in Figure 4. Portions of the ligand molecules were excluded to highlight the following points. All guanine residues at the primary recognition site occupy essentially the same relative position as a result of extensive hydrogen bonding and, with the exception of His39 of RNase Ms (equivalent to His40 of RNase T_1), all active-site residues are almost congruent. Remarkable coplanarity was also observed for base groups stacked on the imidazolium group of H92 at the N1 site, including the guanine of GpcU3, the 3′-end guanine of G2′p5′G, and the cytosine moiety of GfpC. Unlike binding of the guanine moiety at the primary recognition site, the base groups at the N1 subsite are not constrained by hydrogen bonds so that different coplanar orientations of the same base group can occur; e.g., compare the two guanine moieties at this locus in Figure 4. Good overlap was also observed for the phosphate groups of G2′p5′G and GfpC (at site A) but their phosphorus atoms were over 2 Å distant from that in the phosphonate group of GpcU1, which is considerably displaced at the p1 subsite to site B.

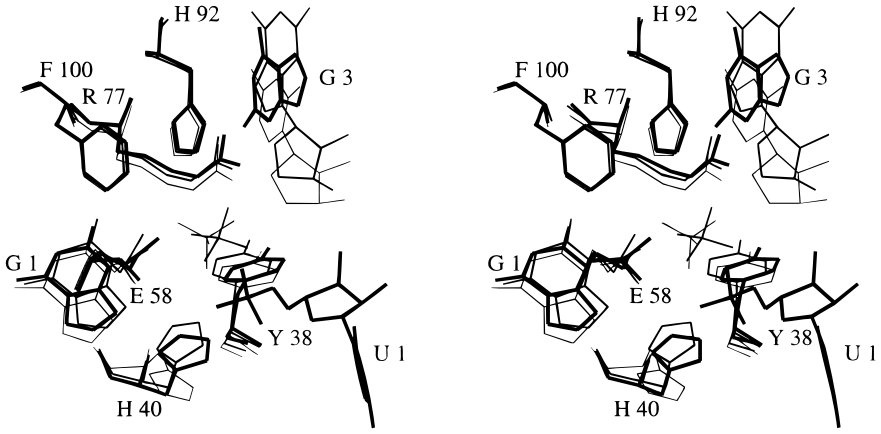

FIGURE 4: Superpositioning of active-site residues and ligand portions for RNase T_1−GpcU1/3, RNase T_1−G2′p5′G, and RNase Ms−GfpC complexes. Thick, medium, and thin lines represent RNase T_1−GpcU1/3, RNase T_1−G2′p5′G, and RNase Ms−GfpC complexes, respectively. For clarity the 5′-end guanosine ribose group was not included. Only the guanine (G3) of GpcU3 is shown and G1 refers to this moiety on GpcU1. The 5′-carbons of the 3′-end nucleosides are not shown for G2′p5′G and GfpC. The phosphate groups of G′2′p5′G and GfpC at site A are illustrated by the overlapping tetrahedral figures in the middle of this view, which are displaced from the phosphonate group at of the 6′-deoxyuridine 6′-phosphonate fragment (U1) of GpcU1 at site B. The active-site residues are all numbered according to the RNase T_1 sequence.

Table 3: *B*-Factors for Different Moieties of Dinucleoside Monophosphate Substrate Analogues and Guanine Nucleotides from Crystal Structures of Their Complexes with RNase T_1 or RNase Ms

	B-factors (Å^2 ± SD)[b]				
	5′-end nucleoside		phosphor(on)yl group,	3′-end nucleoside	
ligand[a]	guanine	sugar	$PO_2(PO_3)$	sugar	base
GpcU1	5.6 ± 2.8	16.1 ± 3.6	24.1 ± 1.7	29.3 ± 4.4	28.2 ± 4.2
GpcU2	9.5 ± 2.8	16.8 ± 2.5	27.0 ± 4.8	30.9 ± 2.5	38.0 ± 1.2
GpcU3	22.8 ± 4.4	22.0 ± 2.6	19.4 ± 1.7	22.2 ± 2.9	20.5 ± 3.3
GfpC (*13*)	20.6 ± 1.5	27.4 ± 5.4	25.3 ± 3.6	33.8 ± 3.0	30.5 ± 2.8
G2′p5′G (*12*)	22.3 ± 1.6	29.8 ± 0.8	31.4 ± 0.3	29.6 ± 0.6	27.0 ± 0.6
3′-GMP (*6*)	12.4 ± 1.8	25.4 ± 3.2	32.2 ± 2.5		
3′-GMP (*7*)	16.0 ± 2.3	35.5 ± 5.4	47.2 ± 1.7		
3′-GMP (*8*)	12.4 ± 2.8	28.3 ± 6.0	48.9 ± 2.6		
3′-GMP[c] (*9*)	29.1 ± 1.7	40.3 ± 2.5	45.9 ± 0.5		
3′-GMP[d] (*9*)	18.2 ± 1.8	23.6 ± 2.0	26.7 ± 1.1		
2′-GMP (*23*)	15.3 ± 1.1	21.2 ± 0.8	22.5 ± 0.4		

[a] Suffixes 1, 2, and 3 for GpcU refer to ligands with guanine groups bound at the primary recognition site of protein molecule A, the primary recognition site of protein molecule B, and the N1 subsite of protein molecule A, respectively. Numbers in parentheses are references. Data for GfpC and G2′p5′G are for major conformers only. [b] Average *B*-factors were calculated for all atoms in each moiety; bridging atoms in the ester linkages were considered as part of the sugars; nonbridging phosphorus-bound oxygens were considered part of the phosphonate (PO_2) and phosphate (PO_3) groups. [c] Conformation of 3′-GMP with the phosphate group at site A. [d] Conformation of 3′-GMP with the phosphate group at site B.

Dynamics of Bound Ligands. Heterogeneity of *B*-factors was observed that correlated with base, sugar, and phosphonate/phosphate segments of the bound ligands as shown in Table 3. In the cases of GpcU1, GpcU2, and 3′-GMP, *B*-factors for the guanine, guanosine−ribose, and phosphonate moieties are inversely proportional to the number of hydrogen bonds involved in binding each segment. [The relationship of B-factors with protein−ligand hydrogen bonding was recently reported for glycoside binding with concanavalin A (*36*).] The higher *B*-factors for GpcU3 vis à vis those for GpcU1/GpcU2 and their similarity between segments are consistent with the lack of hydrogen bonding between GpcU3 and the protein. The much smaller gradient in *B*-factors for guanine and guanosine−ribose moieties of bound GfpC and G2′p5′G suggests a cooperative dynamic linkage between the guanine and ribose segments that is dependent on their mutual binding. The lower guanine *B*-factors for bound 2′-GMP correlate with those for its more tightly bound phosphate group (*37*).

DISCUSSION

Ligand Interactions at the Active Site Are Not Dependent on the Crystal Structure. In view of the structures of the G2′p5′G−RNase T_1 and GfpC−RNase Ms complexes, it might have been expected that GpcU bound at the active site of RNase T_1 would have its phosphonate group in close proximity with Arg77, His92, and Phe100 at the p1 subsite and that the uracil moiety would be stacked on His92 at the N1 subsite. Therefore, it is possible that the lack of these interactions is a result of crystal packing, particularly since hydrogen bonding between GpcU3 and GpcU2 (in a neighboring asymmetric unit) was shown to be part of the lattice structure. Arguments against this view can be summarized as follows. First, the results in Figure 3 and Table 2 indicate that the two GpcU molecules at their respective active sites have almost identical conformations and hydrogen-bonding characteristics (involving the guanine, guanosine 2′-OH, and phosphonate groups), even though they differ in their local environments regarding the existence of a water−phos-

phonate interaction for GpcU1, the presence of guanine (from GpcU3) stacked on His92 adjacent to GpcU1, and a hydrogen bond between the uridine ribose of GpcU1 and the phosphonate of GpcU3. Second, NMR studies of GpcU binding with orthologous RNase Pb_1 indicated that the uridine moiety was not bound to the enzyme (*16*). Third, alternate minor conformations were observed for bound G2′p5′G with RNase T_1 (*12*) and for gfpC with RNase Ms (*13*) that form fewer hydrogen bonds with the phosphate groups at the p1 subsite and exhibit no interactions at the N1 subsite for guanine and cytosine base groups, respectively. Also, a precedent for the binding mode of the guanylyl moieties of GpcU1/GpcU2 has recently been reported for a RNase T_1 complex with 3′-GMP where its phosphate group only involves hydrogen bonding with Tyr38 at site B (see above). Last, kinetic and mutagenic studies of RNase T_1 with GpN substrates independently suggested that a nonproductive, major binding mode has no interactions of the leaving nucleoside (N) group at the N1 subsite of the enzyme (*3*). Therefore, it is reasonable to conclude that the binding interactions of GpcU1 and GpcU2 with RNase T_1 observed here are not the result of crystal lattice forces and most likely approximate those that occur in solution. The fact that $\Delta G°$ values for GpcU and GpU binding with RNase T_1 are almost the same (see above) suggests that they bind in a similar manner. On the other hand, the binding of GpcU3 at the N1 site to form a tertiary complex with protein molecule A and GpcU1 is obviously stabilized by its bonding with GpcU2 in a neighboring asymmetric unit.

Significance of Guanylyl 2′-OH Group Interactions with His40 and Glu58. Studies on the pH dependence of ligand binding with RNase T_1 comparing a variety of guanosine and deoxyguanosine nucleosides/nucleotides revealed the existence of a binding site for the 2′-OH group and suggested the involvement of a deprotonated carboxyl group and a protonated imidazole group in this interaction (*37*, *38*). Subsequently, a crystal structure of the enzyme complexed with two guanosines was reported and indicated that hydrogen bonds for the guanosine 2′-OH group at the active site involved the side chains of His40 and Asn36; however, modeling of enzyme binding with GpG in the same report predicted that the Guo 2′-OH group (5′-end) was hydrogen-bonded with His40 (donor) and Glu58 (acceptor) (*39*). This prediction was experimentally supported by four independent crystal structures for RNase T_1−3′-GMP complexes (*6*−*9*). In the present study we now show that similar binding of this 2′-OH group also occurs with a more RNA-like substrate analogue.

Even though His40 is not conserved among orthologues of RNase T_1, those with known crystal structures have superposable hydrogen-bond donor groups at this locale, including Thr42 for RNase St and Lys27 for barnase (*13*). In the case of barnase, it had been suggested that Lys27 is functionally analogous to His40 in RNase T_1 (*5*). Non-orthologous enzymes in two additional ribonuclease superfamilies also have Lys residues in this position, with Lys 108 for RNase Rh and Lys41 for RNase A (*13*). In the case of RNase A the crystal structure of its complex with 3′-CMP revealed hydrogen bonding of the ligand 2′-OH group with the ϵ-NH_3^+ group of Lys41 (*40*). In addition, the structure of RNase A−uridine vanadate complexes (an analogue for a likely TBP intermediate/transition state) evidenced a strong interaction of Lys41 with the apical 2′-oxygen (*41*). Therefore, members of three ribonuclease superfamilies catalyzing comparable transesterification reactions have a hydrogen-bond donor (i.e., either imidazolium, hydroxyl, or ammonium groups) in the same region of the active site as the His40 imidazolium group of RNase T_1 and it is possible that these groups share a common functional interaction with the substrate 2′-OH group. Molecular dynamics simulations of substrate interactions with RNase T_1 (*42*) and RNase A (*43*) predicted hydrogen bonding of the 2′-OH group with His40 and Lys41, respectively; in the case of RNase A, it was suggested that this interaction with Lys41 might be required for efficient deprotonation of this substrate group by His12 (*43*). In addition, site-directed mutagenesis studies of His40 of RNase T_1 (*44*), Lys27 of barnase (*45*), and Lys41 of RNase A (*46*) reported a dramatic loss in activity upon substitution, and in all cases where kinetic parameters were determined, this was mainly reflected in k_{cat}, which suggests a role for these residues in transition-state stabilization.

Hydrogen-bond donor interaction might orient the reactive 2′-OH group for more efficient proton transfer to the general base catalyst (i.e., a carboxylate for RNase T_1 and its orthologues; an imidazole for RNase Rh and RNase A). However, in cases where the putative hydrogen-bond donor group is relatively acidic (e.g., His imidazolium or Lys ammonium groups) it is not clear how reprotonation of the nascent alkoxide could be prevented, although this was reported to be theoretically possible in a gas-phase model system for RNase A (*47*). Cooperativity observed for the catalytic action of His40 and Glu58 of RNase T_1 (*44*) might reflect their common hydrogen bonding with the substrate guanylyl 2′-OH group. Whether these interactions are the same for catalytic and noncatalytic substrate binding modes is uncertain.

Comparisons with UpcA, dCpdA, and 3′-CMP Binding with RNase A. UpcA is a substrate analogue for pyrimidine-specific RNase A (or its active derivative RNase S) that corresponds with GpcU for guanine-specific RNase T_1. Coordinates for an unrefined X-ray crystal structure of a RNase S−UpcA complex (*48*) were used to contrast the ligand binding modes for the two enzymes. The uracil moiety of UpcA is bound at the primary recognition site of RNase S; however, unlike the corresponding case for RNase T_1, the adenine moiety occupies the N1 subsite being stacked on the imidazolium group of His119 (putative general acid catalyst) and the phosphonate group "completely" interacts at the p1 subsite. The latter conclusion is strongly supported by the results in Table 4, which compare hydrogen bonding at the active site of RNase S with UpcA and RNase A with 3′-CMP and dCpdA ligands. The uridylyl moiety of UpcA superposes almost congruently with the bound 3′-CMP with all atoms displaced by less than 0.75 Å (data not shown), but no interactions of the uridylyl 2′-OH group with His12 and Lys41 were observed. On the other hand, (P)O atoms of the phosphonate group of UpcA and the phosphate groups of 3′-CMP and dCpdA bind in a similar fashion. It is interesting that the distance between the imidazolium group of His119 and C6′ in the UpcA complex is almost identical to that with a (P)O in the 3′-CMP complex and 5′O in the dCpdA complex (see Table 4). (In contrast, the corresponding distance between His92 and C6′ in the RNase T_1−GpcU complex is 6.9 Å.) These results demonstrate that a phos-

Table 4: Selected Hydrogen-Bond Distances for Active-Site Groups in Complexes of RNase A with UpcA and 3′-CMP

donor[a]		acceptor[a]		distance (Å)		
residue (moiety)	atom	residue (moiety)	atom	UpcA[b]	3′-CMP[c]	dCpdA[d]
Gln11	NE2	PO_2	(P)O	2.94	3.35	2.92
His12	NE2	PO_2	(P)O	3.07	2.68	2.76
Phe120	N	PO_2	(P)O	3.14	2.72	3.07
His119	ND1	A	(5′O)[e]	3.08	3.06	2.67
U/C	2′O	His12	NE2	4.54	2.91	
Lys41	NZ	U/C	2′O	6.97	2.68	
Asn44	ND2	U/C	2′O	3.14	3.61	

[a] PO_2 represents the phosphinic group with two nonbridging oxygens; (P)O is a phosphinic oxygen; U, C, and A are uridine, cytidine, and adenosine/6′-deoxyhomoadenosine, respectively. [b] Coordinates were obtained from ref *48*. [c] PDB code 1rpf (*40*). [d] PDB code 1rpg (*40*). [e] 5′O for dCpdA or its spatially equivalent 6′C in UpcA or P(O) in 3′-CMP.

phonate ester group (on UpcA) and a phosphodiester group (on dCpdA) bind in a similar manner at the p1 subsite of RNase A, which is consistent with the fact that both groups are monoanionic at the pH values used and have a similar calculated negative charge on their (P)O atoms (data not shown).

The above findings suggest that the hierarchy of subsite binding affinities for dinucleoside monophosphate substrates is different for RNase A and RNase T_1 regarding interactions at the primary recognition (guanine or pyrimidine), (guanylyl or pyrimidylyl) 2′-OH, p1, and N1 subsites. Unfortunately, *B*-factors for the RNase A−UpcA complex are not available to corroborate this view, but they are available for the RNase A−dCpdA complex, which reveals a similar overall binding mode of dCpdA with that for UpcA. Unlike the results for GpcU1 and GpcU2 in Table 3, the *B*-factors for dCpdA are considerably more variable for atoms within each moiety; nevertheless, they compare roughly as: PO_2 = cytosine < adenine < deoxyriboses. This order again correlates with the number of hydrogen bonds between the enzyme and each moiety (data not shown) but is dramatically different from the corresponding order for GpcU1 and GpcU2 in Table 3. It is possible that tighter binding of the leaving nucleoside group at the N1 site characterizes RNase A vis à vis RNase T_1 since the adenine group of dCpdA is stabilized by several hydrogen bonds in addition to stacking interactions on the imidazolium (general acid) group, which is common to both enzymes (*32*, *48*; see Figure 4). Therefore, it is likely that RNase T_1 and RNase A differ regarding the relative affinities at the different subsites for dinucleoside monophosphate substrates. It is also noteworthy that the binding of dinucleoside monophosphonate substrate analogues for both enzymes appears to exclude simultaneous, strong interactions at the 2′-OH and p1 subsites that compose the catalytic site.

Implications for the Transesterification Catalytic Mechanism. The results of the present study on the RNase T_1−GpcU complex and previous results on the RNase A−UpcA complex suggest that these phosphonate substrate analogues have the potential to interact optimally with the enzyme at all relevant subsites including the primary recognition site (guanine with RNase T_1 and uracil with RNase A), the 2′-OH subsite (RNase T_1 only),[4] the p1 subsite (for RNase A only), and the N1 subsite (for RNase A only) and are excellent models for ground-state substrate interactions. Since it is axiomatic that enzymes bind optimally with transition states for the catalyzed reaction, we hypothesize that strong interactions of the relevant 2′-OH and phosphate groups only occur with a TBP-like transition state, which explains why neither GpcU nor UpcA binds at all available subsites (i.e., no binding at the p1 and N1 subsites for GpcU with RNase T_1; no binding at the uridylyl 2′-OH subsite for UpcA with RNase A). This suggestion implies that catalytic groups at the p1 subsite of RNase T_1 are stabilized for transition-state binding and this is evidenced by their fixed positions (held by side-chain−main-chain hydrogen bonding; see Table 2) in the free enzyme and a variety of complexes as recently noted (*9*). The observation of alternate binding modes for the phosphomonoester group of 3′-GMP (*9*, *26*) and the phosphodiester groups of GF2′p5′G (*12*) and GfpC (*13*) also supports this hypothesis.

The "exit" conformation of the 3′-GMP (i.e., phosphate bound at site B) hydrolysis product of *exo*-(S_p)-guanosine 2′,3′-cyclophosphorthiolate is essentially the same as that for the guanylyl moiety of GpcU at the active site. This observation suggests that the GpcU complex might represent a preferred "entry" conformation for a dinucleoside monophosphate (GpU) substrate. In this regard, the protonation state of these exit and entry modes would be the same with Glu58 and His92 side chains in their anionic and cationic forms, respectively. Therefore, it is possible that there is a preferred sequence of GpN substrate interactions with the enzyme that first involves strong hydrogen bonding with the guanosine moiety (base and 2′-OH groups) and the phosphate with Tyr38 prior to interaction of the leaving nucleoside group at the N1 subsite, which promotes the TBP transition state at the p1 subsite via interactions with Arg77, His92, and Phe100. Advancement to the transition state might involve continued interaction of the phosphate group with Tyr38, which possibly acts as a "snare" to guide this process. Such a role would be consistent with the exclusive effect of a Tyr38Phe mutant on k_{cat} (*3*). The observation of a hydrogen bond of Tyr38 with Asn36 in the present study (Table 2) suggests the possibility of a more concerted process in achieving the transition state since the latter residue was previously proposed to interact with the ribose at the N1 subsite (*3*).

Summary. The following tentative conclusions are supported by the results of the present study. (1) GpcU binding at the active site of RNase T_1 involving the guanine moiety (hydrogen-bonded with Asn43, Asn44, Tyr45, Glu46, and Asn98), the guanosine 2′-OH group (hydrogen-bonded with His40 and Glu58), and the phosphonate (hydrogen-bonded with Tyr38 only) is essentially the same as that for the major binding mode of the substrate, GpU. (2) This substrate binding mode facilitates catalysis by decreasing the mobility (and/or optimizing the orientation) of the phosphate and 2′-OH groups along the reaction coordinate. (3) Maximal interaction of the substrate's guanosine 2′-OH and phosphate groups is only achieved for the TBP intermediate/transition

[4] Different interactions at the 2′-OH subsite for RNase T_1 and RNase A were previously evidenced in ribose/deoxyribose nucleotide binding studies. It was found that the affinity of RNase T_1 with 3′-GMP is considerably greater than that for 3′-dGMP (*37*) but the opposite was true for RNase A, where its affinity with 3′-dUMP is significantly greater than that for 3′-UMP (*49*).

state, which is stabilized by interaction of the leaving nucleoside moiety at the N1 subsite.

REFERENCES

1. Irie, M. (1997) RNase T_1/RNase T_2 Family RNases, in *Ribonucleases: Structures and Functions* (D'Alessio, G., and Riordan, J. F., Eds. Academic Press, Inc., New York, pp 101−130.
2. Pace, C. N., Heinemann, U., Hahn, U., and Saenger, W. (1991) Ribonuclease T1: Structure, Function, and Stability, *Angew. Chem., Int. Ed. Engl. 30*, 343−360.
3. Steyaert, J. (1997) A Decade of Protein Engineering on Ribonuclease T_1: Atomic Dissection of the Enzyme−Substrate Interactions, *Eur. J. Biochem. 247*, 1−11.
4. Sowa, G. A., Hengge, A. C., and Cleland, W. W. (1997) ^{18}O Isotope Effects Support a Concerted Mechanism for Ribonuclease A, *J. Am. Chem. Soc. 119*, 2319−2320.
5. Steyaert, J., Hallenga, K., Wyns, L., and Stanssens, P. (1990) Histidine-40 of Ribonuclease T_1 Acts as a Base Catalyst When the True Catalytic Base, Glutamic 58, is Replaced by Alanine, *Biochemistry 29*, 9064−9072.
6. Zegers, I., Haikal, A. F., Palmer, R., and Wyns, L. (1994) Crystal Structure of RNase T1 with 3′-Guanylic Acid and Guanosine, *J. Biol. Chem. 269*, 127−133.
7. Heydenreich, A., Koellner, G., Choe, H.-W., Cordes, F., Kisker, C., Schindelin, H., Adamiak, R., Hahn, U., and Saenger, W. (1993) The Complex Between Ribonuclease T1 and 3′-GMP Suggests Geometry of Enzymic Reaction Path: an X-ray Study, *Eur. J. Biochem. 218*, 1005−1012.
8. Gohda, K., Oka, K.-I., and Hakoshima, T. (1994) Crystal Structure of RNase T1 Complexed with the Product Nucleotide 3′-GMP: Structural Evidence for Direct Interaction of Histidine 40 and Glutamic Acid 58 with the 2′-Hydroxyl Group of the Ribose, *J. Biol. Chem. 269*, 17531−17536.
9. Zegers, I., Loris, R., Dehollander, G., Haikal, A. F., Poortmans, F., Steyaert, J. and Wyns, L. (1998) Hydrolysis of a Slow Cyclic Thiophosphate Substrate of RNase T1 Analyzed by Time-Resolved Crystallography, *Nat. Struct. Biol. 5*, 280−283.
10. Walz, F. G., Jr., and Terenna, B. (1976) Subsite Interactions of Ribonuclease T_1: Binding Studies of Dimeric Substrate Analogues, *Biochemistry 15*, 2837−2842.
11. Walz, F. G., Jr. (1997) Upstream Subsite Interactions for Oligonucleotide Binding with Ribonuclease T_1, *Biochim. Biophys. Acta 1350*, 183−188.
12. Koepke, J., Maslowska, M., Heinemann, U., and Saenger, W. (1989) Three-Dimensional Structure of Ribonuclease T_1 Complexed with Guanylyl-2′, 5′-guanosine at 1.8 Å Resolution, *J. Mol. Biol. 206*, 475−488.
13. Nonaka, T., Nakamura, K. T., Uesugi, S., Ikehara, M., Irie, M., and Mitsui, Y. (1993) Crystal Structure of Ribonuclease Ms (as a Ribonuclease T_1 Homologue) Complexed with a Guanylyl-3′,5′-Cytidine Analogue, *Biochemistry 32*, 11825−11837.
14. Shibata, Y., Shimada, I., Ikehara, M., Miyazawa, T., and Inagaki, F. (1988) ^1H NMR Investigation of the Interaction between RNase T_1 and a Novel Substrate Analogue, 2′-Deoxy-2′-Fluoroguanylyl-(3′−5′)-Uridine, *FEBS Lett. 235*, 237−240.
15. Baudet, S., and Janin, J. (1991) Crystal Structure of a Barnase−d(GpC) Complex at 1.9 Å Resolution, *J. Mol. Biol. 219*, 123−132.
16. Yakovlev, G. I., and Moiseyev, G. P. (1993) NMR Studies of a Complex of RNase *Penicillium brevicompactum* with Dinucleoside Phosphonate and the Implications for the Mechanism of Enzyme Action, *Biochim. Biophys. Acta 1202*, 143−148.
17. Kreitman, R. J., and Walz, F. G., Jr. (1983) Ribonuclease T_1 Binds with an Isosteric Non-Active Phosphonate Analogue of GpU, *Biophys. J. 41*, 390a.
18. Jones, G. H., Albrecht, H. P., Damodara, N. P., and Moffat, J. G. (1970) Synthesis of Isosteric Phosphonate Analogues of Some Biologically Important Phosphodiesters, *J. Am. Chem. Soc. 92*, 5510−5511.
19. Jones, G. H., and Moffat, J. G. (1968) The Synthesis of 6′-Deoxyhomonucleoside 6′-Phosphonic Acids, *J. Am. Chem. Soc. 90*, 5337−5338.
20. Montgomery, J. A., Thomas, H. J., Kisliuk, R. L. and Gaumont, Y. (1979) Phosphonate Analogue of 2′-Deoxy-5-fluorouridylic Acid, *J. Med. Chem. 22*, 109−111.
21. Green, D. P., Ravindranathan, T., Reese, C. B., and Saffhill, R. (1970) *Tetrahedron 26*, 1031−1041.
22. Chládek, S., and Smrt, J. (1964) Oligonucleotidic Compounds. VIII. Synthesis of Adenylyl-(5′→3′)-Uridine, Adenylyl-(5′→3′)-Cytidine, Guanylyl-(5′→3′)-Uridine, Guanylyl-(5′→3′)-Cytidine, Cytidylyl-(5′→3′)-Cytidine, Adenylyl-(5′→3′)-Uridylyl-(5′→3′)-Cytidine and Related Compounds, *Collect. Czech. Chem. Commun. 229*, 214−233.
23. Rammler, D. H., and Khorana, H. G. (1962) Studies on Polynucleotides. XVI. Specific Synthesis of the $C_{3'}-C_{5'}$, Interribonucleotidic Linkage. Examination of Routes Involving Protected Ribonucleosides and Ribonucleoside 3′-Phosphates. Synthesis of Uridylyl-(3′→5′)-Adenosine, Uridylyl-(3′→5′)-Cytidine, Adenylyl-(3′→5′)-Adenosine, and Related Compounds, *J. Am. Chem. Soc. 84*, 3112−3122.
24. Walz, F. G., Jr., and Hooverman, L. L. (1973) Interaction of Guanine Ligands with Ribonuclease T_1, *Biochemistry 12*, 4846−4851.
25. Zabinski, M., and Walz, F. G., Jr. (1976) Subsites and Catalytic Mechanism of Ribonuclease T_1: Kinetic Studies Using GpC and GpU as Substrates, *Arch. Biochem. Biophys. 175*, 558−564.
26. Walz, F. G., Jr. (1992) Relaxation Kinetics of Ribonuclease T_1 Binding with Guanosine and 3′-GMP, *Biochim. Biophys. Acta 1159*, 327−334.
27. McPherson, A. (1982) *The Preparation and Analysis of Protein Crystals*, John Wiley & Sons, Inc., New York.
28. Jancarik, J., and Kim, S−H. (1991) Sparse-Matrix Sampling—A Screening Method for Crystallization of Proteins, *J. Appl. Crystallogr. 24*, 409−411.
29. Higashi, T., (1990) Auto-Indexing of Oscillating Images, *J. Appl. Crystallogr. 23*, 253−257.
30. Arni, R., Heinemann, U., Tokuoka, R., and Saenger, W. (1988) Three-Dimensional Structure of the Ribonuclease T_1*2′-GMP Complex at 1.9 Å Resolution, *J. Biol. Chem. 263*, 15358−13368.
31. Navaza, J. (1994) AMORE—An Automated Package for Molecular Replacement, *Acta Crystallogr. A50*, 157−163.
32. Brunger, A. T. (1992) *X-PLOR, Version 3.1: A System for X-ray Crystallography and NMR*, Yale University Press, New Haven, CT.
33. Jones, T. A., Zou, J. Y., Cowan, S. W., and Kjeldgaard, M. (1991) Improved Methods for Building Protein Models in Electron Density Maps and the Location of Errors in These Models, *Acta Crystallogr. A47*, 110−119.
34. Laskowski, R. A., MacArthur, M. W., Moss, D. S., and Thornton, J. M. (1993) PROCHECK—A Program to Check the Stereochemical Quality of Protein Structures, *J. Appl. Crystallogr. 26*, 283−291.
35. Walz, F. G., Jr., Osterman, H. L., and Libertin, C. (1979) Base-Group Specificity at the Primary Recognition Site of Ribonuclease T_1 for Minimal RNA Substrates, *Arch. Biochem. Biophys. 195*, 95−102.
36. Bradbrook, G. M., Gleichmann, T., Harrop, S. J., Habash, J., Raftery, J., Kalb, J., Hillier, I. H., and Helliwell, J. R. (1998) X-ray and Molecular Dynamics Studies of Concanavalin-A Glucoside and Mannoside Complexes, *J. Chem. Soc., Faraday Trans. 94*, 1603−1611.
37. Walz, F. G., Jr. (1977) Studies on the Nature of Guanine Nucleotide Binding with Ribonuclease T_1, *Biochemistry 16*, 5509−5515.
38. Walz, F. G., Jr. (1976) Ribose Recognition by Ribonuclease T_1: Difference Spectral Binding Studies with Guanosine and Deoxyguanosine, *Biochemistry 15*, 4446−4450.
39. Lenz, A., Cordes, F., Heinemann, U., and Saenger, W. (1991) Evidence for a Substrate-Binding Subsite in Ribonuclease T_1, *J. Biol. Chem. 266*, 7661−7667.

40. Zegers, I., Maes, D., Dao-Thi, M.-H., Poortmans, F., Palmer, R., and Wyns, L. (1994) The Structures of RNase A Complexed with 3′-CMP and d(CpA): Active Site Conformation and Conserved Water Molecules, *Protein Sci. 3*, 2322−2339.
41. Wladowski, B. D., Svensson, L. A., Sjolin, L., Ladner, J. E., and Gilliland, G. L. (1997) Structure (1.3 Å) and Charge States of a Ribonuclease A−Uridine Vanadate Complex: Implications for the Phosphate Ester Hydrolysis Mechanism, *J. Am. Chem. Soc*. *120*, 5488−5498.
42. Cordes, F., Starikov, E. B., and Saenger, W. (1995) Initial State of an Enzymatic Reaction. Theoretical Prediction of Complex Formation in the Active Site of RNase T1, *J. Am. Chem. Soc*. *117*, 10365−10372.
43. Haydock, K., Lim, C., Brunger, A. T., and Karplus, M. (1990) Simulation Analysis of Structures on the Reaction Pathway of RNase A, *J. Am. Chem. Soc*. *112*, 3826−3831.
44. Steyaert, J., and Wyns, L. (1993) Functional Interactions Among the His40, Glu58 and His92 Catalysts of Ribonuclease T_1 as Studied by Double and Triple Mutants, *J. Mol. Biol*. *229*, 770−781.
45. Mossakowska, D. E., Nyberg, K., and Fersht, A. R. (1989) Kinetic Characterization of the Recombinant Ribonuclease from *Bacillus amyloliquefaciens* (Barnase) and Investigation of Key Residues in Catalysis by Site-Directed Mutagenesis, *Biochemistry 28*, 3843−3850.
46. Trautwein, K., Holliger, P., Stackhouse, J., and Benner, S. A. (1991) Site-Directed Mutagenesis of Bovine Pancreatic Ribonuclease: Lysine-41 and Aspartate-121, *FEBS Lett*. *281*, 275−277.
47. Lim, C., and Tole, P. (1992) Endocyclic and Exocyclic Cleavage of Phosphorane Monoanion: A Detailed Mechanism of the RNase A Transphosphorylation Step, *J. Am. Chem. Soc. 114*, 7245−7252.
48. Richards, F. M., and Wyckoff, H. W. (1973) 1 Ribonuclease-S, in *Atlas of Molecular Structure in Biology* (Philips, D. C., and Richards, F. M. (Eds.) Oxford University Press, London.
49. Walz, Jr., F. G. (1971) Kinetic and Equilibrium Studies on the interaction of Ribonuclease A and 2′-Deoxyuridine 3′-Phosphate, *Biochemistry 10*, 2156−2162.

BI982612Q